

Composite Advanced Detection for Coal Seam Thickness in Coal Roadway

Wang Bo^{1,2}, Zhang Xiayang^{1,2}, Liu Shengdong^{1,2,*}, Lu Tuo^{1,2} and Chen Mulan¹

¹State Key Laboratory of Deep Geomechanics & Underground Engineering, China University of Mining & Technology, Xuzhou 221008, China; ²School of Resources and Earth Science, China University of Mining & Technology, Xuzhou 221008, China

Abstract: The thickness change of coal seam can be resulted from several reasons, like primary sedimentary environment and later tectonic deformation. The thickness change ahead of driving face may have an impact on the efficiency and safety of the mining progress, thus the advanced prediction of seam thickness is important. However, it is hard to predict the seam thickness with a single advanced detection method. This paper combines three methods, e.g., MSP, MRP, and MTEM to perform a joint detection, and makes data fusion through wavelet analysis, which makes use of the elastic wave field and geo-electrical field characteristics. A field test indicates that the prediction of seam thickness by means of integrated advanced detection is approximately accurate with an error less than 5%.

Keywords: Coal roadway, composite detection, elastic wave field, geo-electrical field, wavelet analysis.

1. INTRODUCTION

The thickness change of coal seam is principally affected by the fold structure, fracture structure and magmatic intrusion [1]. Deployment and mining of coal mining face is influenced by the thickness variation [2]. Meanwhile, the thickness mutation site is usually the gas accumulation abnormal area, which threatens the safety production of mine [3]. At present, in the laneway, exploring coal seam thickness depends on drilling and lane detection whose disadvantage is short distance, low efficiency. Rapid forecasting coal seam thickness by geophysical method is actual demand for coal mine production departments [4-6].

The thickness change ahead of tunnel face represents different physical properties and geological conditions in each case. First, the observing system of different physical detection methods varies because the detecting line, detecting point and the detected target are on the same line [7, 8]. Second, the anomaly received by the advanced detection comes from an integrated whole-space response [9]. Besides the anomaly from ahead, it is likely that it is caused by the lateral influence of non-detected objects. Third, predicting coal seam change needs not only the structure information of the changing point, but also the physical property indications of the coal seam thickness. Therefore, this paper adopts seismic reflection method combining with exploration data of geo-electrical field to perform the advanced detection of coal seam thickness.

2. PRINCIPLE

Characteristics of coal seam are low velocity and low density. In the light of the principle of wave impedance, the average density is 1.8g/cm^3 for the coal seam and 2.6g/cm^3 for the wall rock. The average P-wave velocity is 2.0m/ms

for the coal seam and 3.5m/ms for wall rock. The reflection coefficient is approximately 0.46, therefore interface between coal seam and wall rock are a strong reflected interface, which is beneficial to employ MSP (Mine Seismic Prediction) to predict the coal-rock interface. On account of reflected wave exploration theory that the seismic wave which meets with the geological interfaces form reflection, sources and receivers are fixed on the wall of roadway. The receiving seismic record is processed by wave field separation, velocity analysis and migration imaging to achieve the forecast of front interfaces with reflected energy profile.

The resistivity of various rock stratum is significant difference in the coal mine. For example, the resistivity of blind coal is about $300\Omega\cdot\text{m}$, while the resistivity of wall rock is approximately $100\Omega\cdot\text{m}$. In the vertical direction, the coal seam thickness variation leads to the rate between coal seam and rock stratum changes. When the coal-rock rate increases, appear resistivity increases. On the contrary, the depressed rate brings to the low resistivity. Therefore, MRP (Mine Resistivity Prediction) and MTEM (Mine Transient Electromagnetic Method) which both based on the difference of resistivity are used to detect the coal seam variation. According to the principle of electrical prospecting, 64 electrodes are placed on the laneway floor. Source electrode A slides backwards one after another from tunnel face, and electrode B lies beyond 3~5 times of measuring line length away. Based on the measured data MRP applies superposition operation to predict the front the thickness abnormality with apparent resistivity contour map. MTEM makes use of secondary induced signal which measured by multi-turn receiver loop on the tunnel face. By apparent resistivity calculation and time-depth conversion, the abnormality can be forecasted with apparent resistivity contour map.

So far, there is no complete theoretical system with respect to efficient fusion arithmetic of multi-data fusion. However, in many fields, plenty of mature and effective fu-

*Address correspondence to this author at the University Road, Xuzhou, China. Postcard: 221008; Tel: +86 51683995678; E-mail: wbsyes@126.com

sion methods have been put forward in accordance with their specific application backgrounds [10-14]. This paper uses wavelet theory for data fusion. All types of information are decomposed as wavelets, and adjustments are made for detailed and approximate sections at the same scale. For detailed section (energy anomaly interface), the principle of maximum absolute value is adopted, and for approximate section (apparent resistivity), weighted average is calculated. Finally, the data fusion can be achieved.

3. ENGINEERING APPLICATION

3.1. Geologic Aspects

In a coal mine in Luoyang, China, the great change of coal thickness of the lower part of Shanxi formation brings trouble to laneway driving, which is realistic demand to ascertain the thickness changes in front of tunnel face. In 12011 working face, contact alley +128m is tunnel face, and front 100m is detection zone. In the detection area, hydrogeology condition is simple and water-bearing content is low. Faults are undeveloped and coal seam change is mainly influenced by sedimentary environment. Meanwhile, there is no laneway in the peripheral areas.

3.2. MSP

2 receivers were installed on the wall of roadway, and 24 sources shot. After filtering the rear wave field by F-K filtering, depth migrated was obtained with uniform direct S wave velocity ($v=1722\text{m/s}$), and anterior reflected energy profile is

seen in Fig. (1). As shown, in the range of 100m in the front of tunnel face, names of the 2 main reflection anomaly interfaces are R1 and R2 respectively, and distance ahead of tunnel face are 10m and 78m respectively.

3.3. MRP

64 electrodes whose interval is 2.5m were placed on the floor of roadway. The current electrode A supplies from 1 to 64, with each power supplying 2s and sampling interval being 50ms. The other 63 non source electrodes simultaneously measure the voltage difference with electrode N which was set in the middle of measuring line. Rear interference signal is filtered by geometric focusing method [15] in accordance with geological data. The pole-dipole apparent resistivity curves of first 6 source electrodes A are migrated to obtain the apparent resistivity section of superposition, which is seen in Fig. (2). It can be seen that there is relatively high resistivity zone with 10m~66m ahead of tunnel face, and the apparent resistivity value is above $60\Omega\cdot\text{m}$. On the basis of DC electrical method of advanced detection, it can be deduced that there may be a high resistivity anomaly in that region.

3.4. MTEM

11 measured points of MTEM was arranged in the tunnel face. The detector was designed as an overlapped loop line with multi-turns of $1.5\text{m}\times 1.5\text{m}$, and the turn of transmitting and receiving coil is 9, 18 respectively. The receiving signal

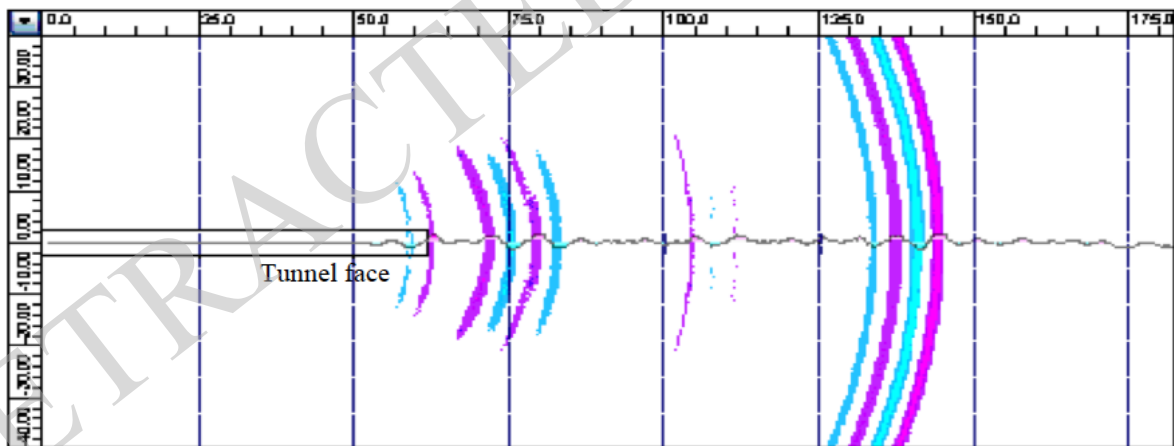


Fig. (1). Prestack depth migration section of MSP.

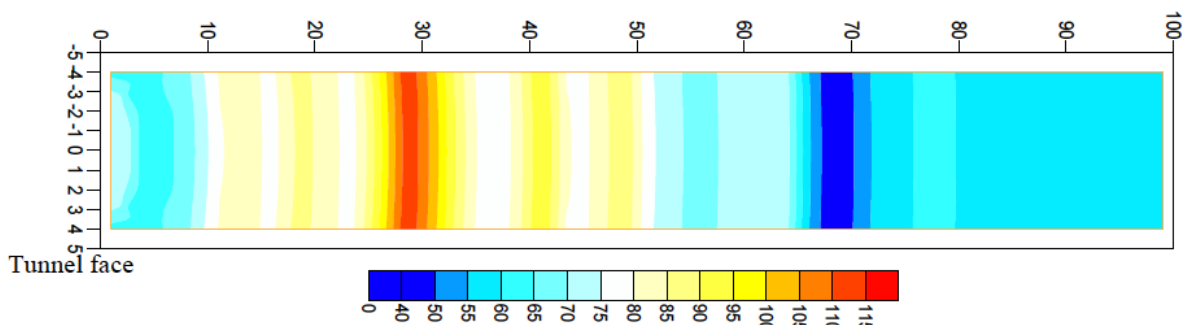


Fig. (2). Apparent resistivity profile map of MRP.

was processed with apparent resistivity calculation and time-depth conversion, result shown as Fig. (3). The detected blind zone is 0~8m in the front of the tunnel face. Within 8~100m, there is a relatively high-resistivity area in the section of 12~70m, and apparent resistivity is above $60\Omega\cdot m$.

3.5. Data Fusion

3.5.1. MRP and MTEM

The processing of MRP and MTEM data can be carried out in several steps. First, the data have to be selected. MTEM data distortion occurs because of signal aberrance during early period, so there will be a detection blind zone at 0~8m ahead of the tunnel face. Thus the front 8m data has to be removed. Then the rest data can be interpolated and decomposed as wavelets, adopting the maximum of absolute value for detailed section, and using weighted average for approximate section. At last, the data fusion can be made, and the map is shown in Fig. (4).

The profile indicates that the apparent resistivity within an area of 12-66m ahead of the tunnel face is above $40\Omega\cdot m$, which suggests a high-resistance anomaly may exist within the area. Therefore, it can be concluded that the fusion makes full use not only of the volume effect of the MRP, but also of the directivity of MTEM, and the region of anomaly can be located more accurately.

3.5.2. MSP, MRP and MTEM

According to the characteristics of the seismic data, the corresponding seismic amplitude values which located in central line in the front 100 seismic migration section is selected, and the amplitude is data of normalization processing.

Taking chosen seismic data as energy signal which is decomposed by wavelet analysis, and selecting DB2 wavelet for processing. 5 layers wavelet decomposition and reconstitution is done by using DB2 wavelet. Low frequency reconstitution is as shown in Fig. (5a), high frequency reconstitution as shown in Fig. (5b). In Fig. (5a), the first layer of the low frequency reconstruction signal is ya1, the second layer of the low frequency reconstruction signal is ya2 and so on. Since the signal of ya5 and ya5 are not obvious, ya4 and ya4 are chose for analysis (as shown in Fig. 5c).

Through comparison result of seismic segmentation in Fig. (5c), in several interfaces, it is all shown that ya4 is a minimum, or a relative minimum “negative sign”, yd4 is a maximum “positive sign”. It can make an integral division for Fig. (4) based on the seismic segmentation information with 6 interfaces. The average of apparent resistivity between 2 interfaces is calculated, shown as Fig. (6).

Fig. (4) is a profile map of apparent resistivity, it embodies the features of MRP and MTEM with the apparent resistivity, and it displays the seismic information with the interface. In Fig. (6), it fuses the information of MSP, MRP and MTEM.

The measured section as shown in Fig. (7), it appears the information of actual coal thickness change, which shows that the fusion result conforms to the practical mining.

CONCLUSION

The advanced detected data of DC and TEM was operated jointly to obtain the comprehensive apparent resistivity profile, which have the features of volume effect of the MRP and the directivity of MTEM.

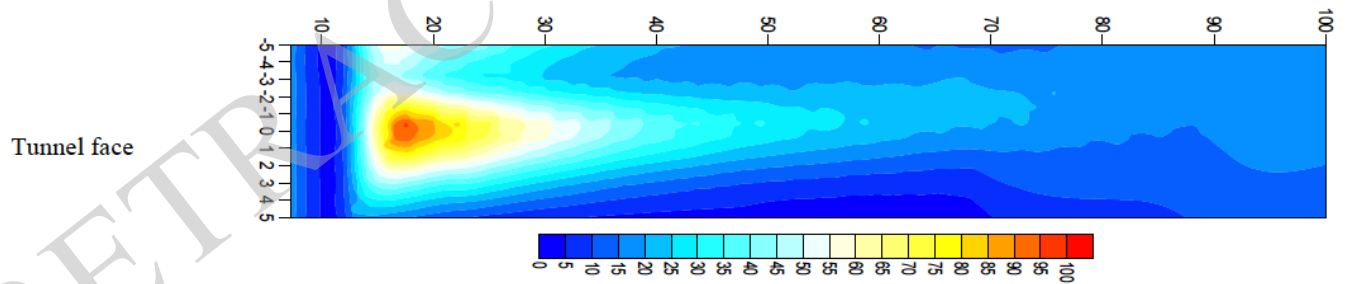


Fig. (3). Apparent resistivity profile map of MTEM.

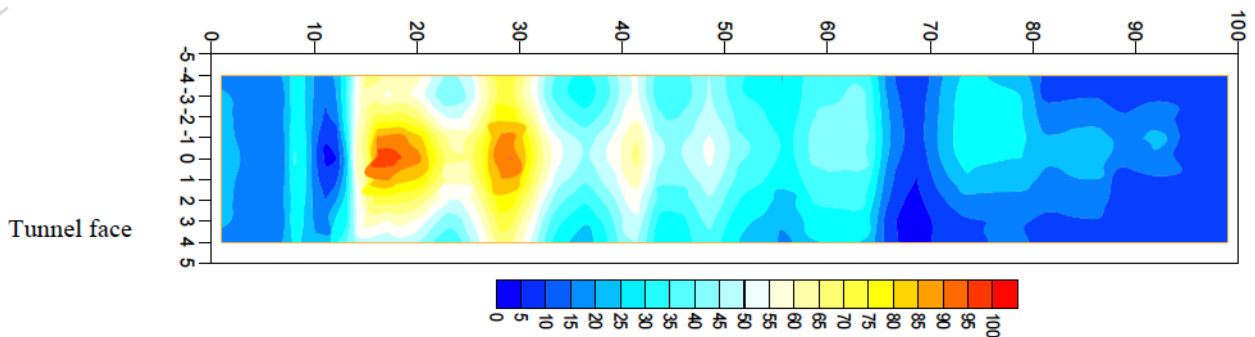
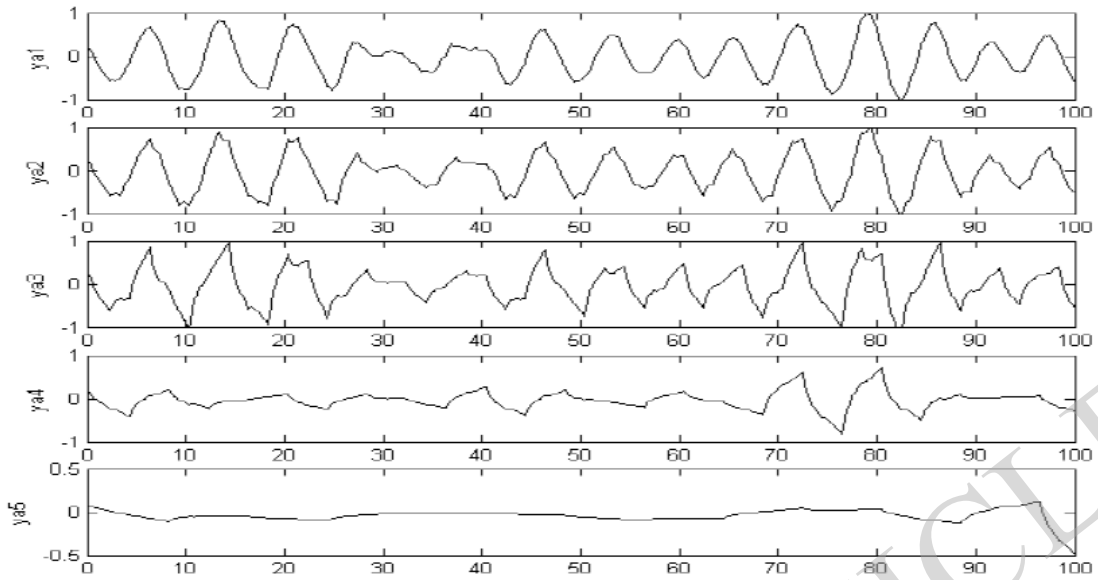
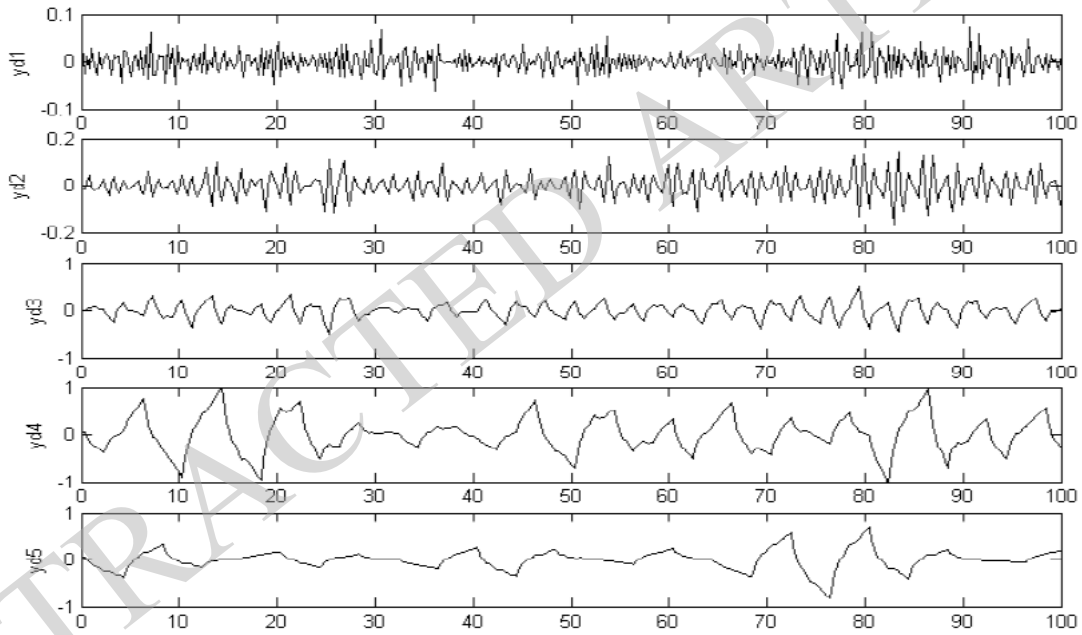


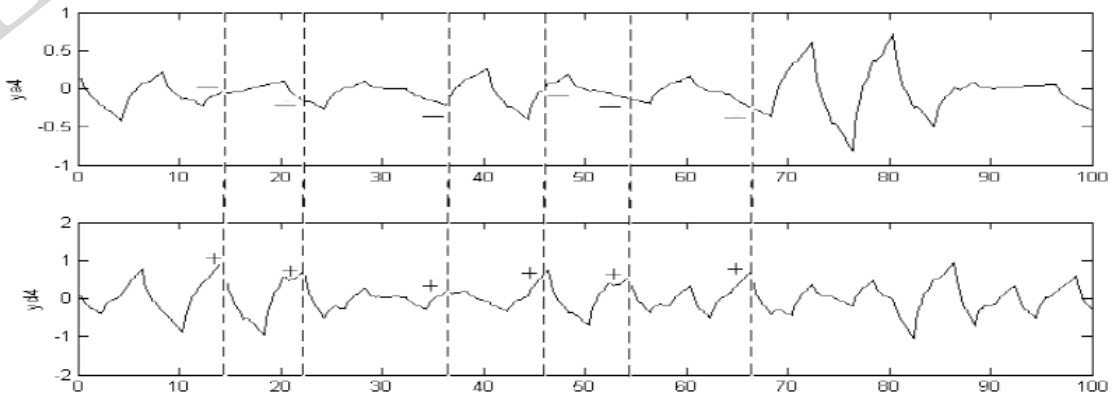
Fig. (4). Fusion image of MRP and MTEM.



(a) Five wavelet layers of low-frequency reconstruction.



(b) Five wavelet layers of high-frequency reconstruction.



(c) The fourth layer low-frequency and high-frequency reconstruction.

Fig. (5). Wavelet analysis of MSP.

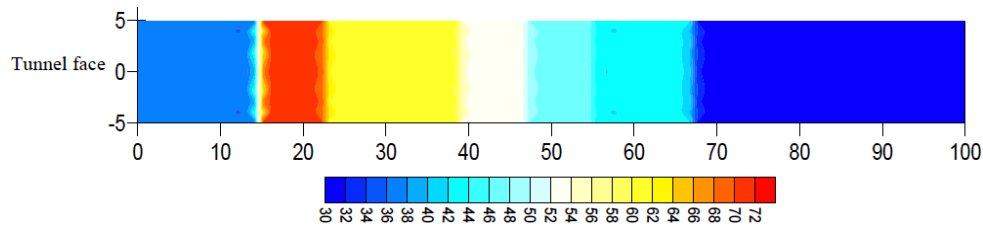


Fig. (6). Fusion image of MSP, MRP and MTEM.

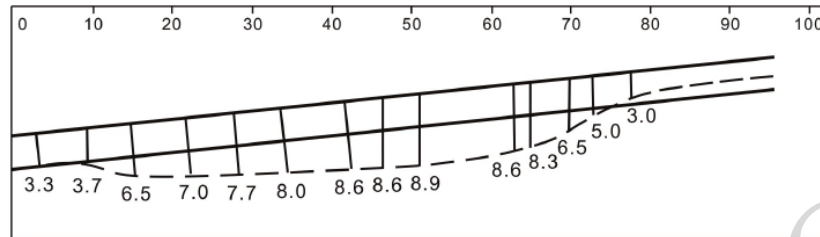


Fig. (7). Measured profile of coal seam thickness.

The energy abnormality signal of MSP was processed by wavelet analysis. Minimal value of low-frequency and maximum value of high-frequency were united to ascertain the seismic interfaces. The comprehensive apparent resistivity profile of MRP and MTEM and the seismic interfaces were associated to form the fusion image. The image agrees with the fact, which indicates the coal seam thickness can be forecasted by advanced prediction method of joint inversion in mine roadway.

CONFLICT OF INTEREST

The authors confirm that this article content has no conflict of interest.

ACKNOWLEDGEMENTS

This research was supported by the Joint Funding Project of National Natural Science Foundation and ShenHua Group Corporation Ltd (U1261202), National Natural Science Foundation Project (51174193, 51374203, 51323004, 41474122).

REFERENCES

- [1] S.Z. Shi, F.B. Li, P. Liang, and Y. Li, "Application of multi-well constrained seismic inversion in quantitative prediction of coal seam thickness", *Journal of Mining and safety engineering*, vol. 28, pp. 328-332, June 2011.
- [2] P. Chen, and G.B. Yin, "Impact of thrust nappe structure on coal seam thickness and its stability in Fufeng of Huainan", *China Coal*, vol. 39, pp. 38-41, 2013.
- [3] J.C. Pashin, "Variable gas saturation in combed methane reservoirs of the Black Warrior Basin: implications for exploration and production", *International Journal of Coal Geology*, vol. 82, pp. 135-146, 2010.
- [4] S.P. Peng, G.G. ZOU, and Q.L. LI, "Seam thickness prediction methods based on the logging constrained seismic inversion", *Journal of China University of Mining and Technology*, vol. 37, pp. 729-733, November 2008.
- [5] Z. Yang, M.C. Ge, and S.G. Wang, "Characteristics of transmitting channel wave in a coal seam", *Mining Science and Technology*, vol. 19, pp. 331-336, 2009.
- [6] Y.M. Du, and C.G. Zhang, "Study of Advance Detection of Coal Seam Thickness based on Integrate Geophysical Prospecting Techniques", *Mining Safety and Environment Protection*, vol. 40, pp. 63-66, 2013.
- [7] Z.X. Liu, Z.H. Yue, and Y.G. Liu, "Application of sector detection technology in advanced detection", *Journal of China University of Mining and Technology*, vol. 36, pp. 822-825, 2007.
- [8] P.S. Zhang, S.D. Liu, and P.G. Li, "Mine transient electromagnetic technology system and its application", *Progress in Geophysics*, vol. 26, pp. 1107-1114, 2011.
- [9] S.H. Zhou, J.C. Yu, and J.H. Chang, "Study of mine transient electromagnetic response characteristics and correction method under support using bolt and wire mesh", *Mining Safety and Environment Protection*, vol. 41, pp. 17-19, June 2014.
- [10] M. Roth, and K. Holliger, "Joint inversion of Rayleigh and guided waves in high-resolution seismic data using a genetic algorithm". In: *Annual Meeting Abstracts, Society of Exploration Geophysicists*, pp. 1570-1573, 1998.
- [11] R.Z. Jing, G.S. Bao, J. Lin, and S.Q. Chen, "A geophysical integration inversion method based on data fusion", *Chinese Journal of Geophysics*, vol. 47, pp. 143-150, May 2004.
- [12] S.P. Sharma, "Appraisal of equivalence and suppression problems in 1D EM and DC measurements using global optimization and joint inversion", *Geophysical prospecting*, vol. 47, pp. 219-249, March 1999.
- [13] R. Chundurur, Z. Zhang, R. Busch, and T. Maher, "Joint inversion of MWD and wire line measurements". In: *Annual Meeting Abstracts, Society of Exploration Geophysicists*, pp. 132-135, 1999.
- [14] M. Peng, H.D. Tan, and M. Jiang, "Three-dimensional joint inversion of magnetotelluric and seismic travel time data with cross-gradient constraints", *Chinese Journal of Geophysics*, vol. 56, pp. 2728-2738, August 2013.
- [15] J.L. Cheng, Y.H. Wang, and S.J. Yu, "The principle and application of advance surveying in roadway excavation by resistivity method", *Coal Geology and Exploration*, vol. 28, pp. 60-62, August 2000.

Received: December 15, 2014

Revised: January 04, 2015

Accepted: February 25, 2015

© Bo et al.; licensee Bentham Open.

This is an open access article licensed under the terms of the Creative Commons Attribution Non-Commercial License (<http://creativecommons.org/licenses/by-nc/3.0/>) which permits unrestricted, non-commercial use, distribution and reproduction in any medium, provided the work is properly cited.